NANO LETTERS

Letter

pubs.acs.org/NanoLett

Nonperturbative Quantum Nature of the Dislocation–Phonon Interaction

Mingda Li,[*,†] Zhiwei Ding,[†] Qingping Meng,[‡] Jiawei Zhou,[†] Yimei Zhu,[‡] Hong Liu,[§] M. S. Dresselhaus,[§,∥] and Gang Chen[*,†]

[†]Department of Mechanical Engineering, MIT, Cambridge, Massachusetts 02139, United States

[‡]Condensed Matter Physics and Material Sciences Department, Brookhaven National Laboratory, Upton, New York 11973, United States

[§]Department of Physics, MIT, Cambridge, Massachusetts 02139, United States

[∥]Department of Electrical Engineering and Computer Sciences, MIT, Cambridge, Massachusetts 02139, United States

Supporting Information

ABSTRACT: Despite the long history of dislocation–phonon interaction studies, there are many problems that have not been fully resolved during this development. These include an incompatibility between a perturbative approach and the long-range nature of a dislocation, the relation between static and dynamic scattering, and their capability of dealing with thermal transport phenomena for bulk material only. Here by utilizing a fully quantized dislocation field, which we called a "dislon", a phonon interacting with a dislocation is renormalized as a quasi-phonon, with shifted quasi-phonon energy, and accompanied by a finite quasi-phonon lifetime, which are reducible to classical results. A series of outstanding legacy issues including those above can be directly explained within this unified phonon renormalization approach. For instance, a renormalized phonon naturally resolves the decade-long debate between dynamic and static dislocation–phonon scattering approaches, as two limiting cases. In particular, at nanoscale, both the dynamic and static approaches break down, while the present renormalization approach remains valid by capturing the size effect, showing good agreement with lattice dynamics simulations.

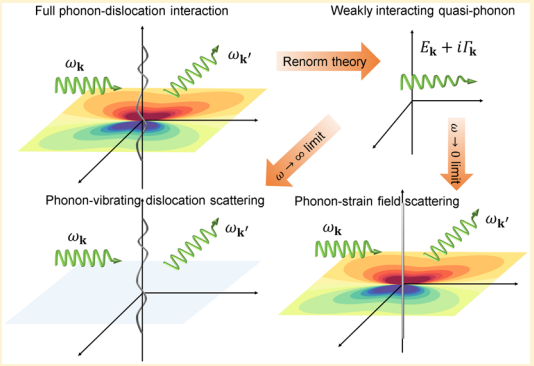

KEYWORDS: *Dislocations, dislocation–phonon interaction, thermal conductivity, phonon transport, effective field theory, renormalization*

A dislocation is a type of line defect within a crystal structure. The presence of dislocations determines the plastic mechanical properties of a material, while it also has widespread influence to the electrical, thermal, and thermoelectric properties of materials.[1] It is well-known that phonons are strongly scattered by crystal dislocations, resulting in dislocation-induced thermal resistivity. However, after over a half-century long dislocation–phonon interaction (DPI) research, starting from the pioneer studies of static anharmonic scattering by Klemens[2] and Carruthers,[3] the understanding of the DPI is still not entirely satisfactory,[4] leaving behind a series of mysteries remaining to be clarified.

The first problem deals with the degree of validity of the perturbation theory, in particular the Born approximation. This issue was pointed out by Carruthers himself as "possibly invalid but still desirable before more sophisticated calculation,"[3] but was often neglected in later developments. To remedy the large quantitative disagreement between the Carruthers' theory and thermal conductivity measurements, such as in a prototype material LiF,[5] later developments gradually adopted an alternative dynamic scattering mechanism.[6−8] However, there is another possibility that the weak DPI comes from the perturbative analysis procedure other than from static strain scattering itself.[3] A weakly interacting approximation, such as the Born approximation, may underestimate the dislocation-induced thermal resistivity. In fact, the Born approximation breaks down in treating the DPI due to the divergence caused by the dislocation's long-range strain field (See Supporting Information A). To the best of our knowledge, a nonperturbative approach has not been implemented in DPI studies to truly capture the long-range nature of this interaction.

The unsatisfactory early developments triggered a second problem, which is a decade-long debate regarding the origin of dislocation–phonon interaction, namely, static strain field scattering[2,9−12] or dynamic vibrating dislocation scattering.[13−18]

This debate is partly due to the similar temperature dependence of the thermal conductivity $k \propto T^{2-3}$ in either scenario, and such a dependence is further limited by only

Received: November 13, 2016
Revised: January 26, 2017
Published: January 31, 2017

DOI: 10.1021/acs.nanolett.6b04756
Nano Lett. 2017, 17, 1587−1594

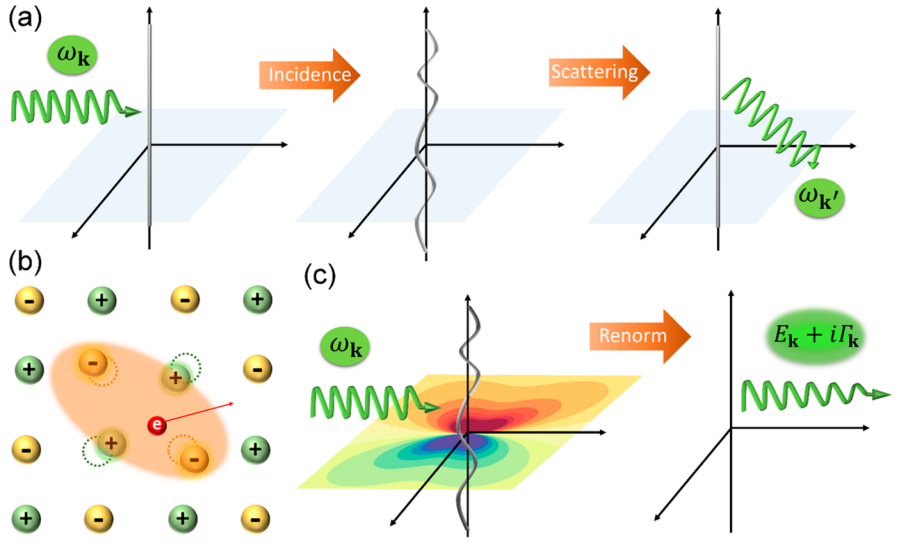

Figure 1. (a) Schematics of classical dynamic dislocation−phonon scattering, where scattering is accomplished when the dislocation absorbs an incoming phonon ω_k and re-emits another phonon $\omega_{k'}$. (b) Due to the electron−ion drag force, an electron is renormalized to a quasi-particle called a "polaron". (c) The quantum picture of the dislocation−phonon interaction. Due to the long-range field of the dislocation, a phonon ω_k starts to interact with the dislocation even far away from the core region, making renormalization a more suitable picture than scattering. After renormalization, the strong DPI disappears. We are left with the weakly interacting quasi-phonons with a renormalized energy E_k and a finite lifetime Γ_k.

Table 1. Brief Comparison between a Phonon and a Dislocation[a]

	phonons	dislocations
essence	small lattice displacement **u**	lattice displacement **u** with topological constraint $\oint d\mathbf{u} = -\mathbf{b}$
energy	kinetic energy + potential energy	kinetic energy + potential energy
interacting with electrons	yes, metallic resistivity	yes, increased resistivity
interacting with a phonon	yes, anharmonicity hence thermal expansion; anharmonicity induced thermal resistivity	yes, dislocation induced thermal resistivity, "fluttering mechanism"
interacting with a dislocation	yes, dislocation induced thermal resistivity	yes, climbing, gliding and pile-up hence polycrystal yield and work hardening
fundamental quantum theory	plenty	dislon theory is one attempt, treating both vibrating dislocation line and long-range strain field from equal footing
nature of quantized modes	plane waves excitation as fluctuation of atomic positions around periodic atomic arrangement	localized waves nearby a dislocation core as fluctuation of atomic positions around a static dislocation
statistics	3D Bosonic quasiparticle	Bosonic quasiparticle in 1D or two independent half-Bosonic quasiparticles in 3D[41]

[a]This provides an intuitive understanding as to why dislocation can and shall be quantized prior to any rigorous math as shown in the main text.

measuring the temperature dependence $k(T)$, which gives little parameter space to fully compare a theory with an experiment. When dynamic scattering occurs, a dislocation starts to vibrate by absorbing a phonon and subsequently emits a phonon (Figure 1a). A consensus gradually formed that a type of viscous dynamic scattering called fluttering plays a significant role in DPI.[4,6,8,17,18] However, the relationship between the static and dynamic scattering is still unclear. In fact, a formalism being able to treat both from an equal footing was still unavailable. What's worse, since both approaches are formulated for bulk materials under thermodynamic limit, what will happen to DPI when the sample size is reduced to nanoscale has been a no man's land.

Third, the dislocation−phonon resonant scattering process can well be described by the Granato−Lücke model where a dislocation is treated as a vibrating string.[15,19,20] However, this simplification fails to describe many features of resonance, such as the phonon polarization dependence, anisotropy, and long-range strain effect.[4,21] In particular, because of the restrictive framework of a classical string, most of the studies until now are limited to the classical elastic wave-dislocation scattering mechanism without referring to a quantized phonon.[14,21−23]

In this study, we show that a quantum field theory of DPI, based on a quantized field of dislocations, called a "dislon",[24] can easily resolve all the above-mentioned problems beyond all expectations (and also solve a few other problems as described below). The vibrating nature coexisting with the long-range strain field of the lattice displacement field of a dislocation makes a quantum-field description of dislocation reasonable. A dislon is similar to a phonon as a type of lattice displacement with both kinetic energy caused by the vibration and potential energy originating from the strain field, yet a dislon exists only near a dislocation core as a collection of localized modes perpendicular to the dislocation line direction, instead of the extended plane waves as the case of a phonon (Table 1). For phonon−dislon interaction, to avoid the uncontrolled expansion in perturbative analysis, an exact functional integral approach is applied, resulting in a renormalized quasi-phonon. The quasi-phonon naturally unifies the static and dynamic DPI having the same origin as the dislon field, where the imaginary

DOI: 10.1021/acs.nanolett.6b04756
Nano Lett. 2017, 17, 1587−1594

part of the quasi-phonon can be reduced to the well-known DPI relaxation time. In particular, since neither the previous static scattering nor the dynamic scattering approach considered the situation of phonon frequency change in a confined environment, but only took into account the scattering between bulk phonons, they both are not capable of dealing with the thermal transport in a dislocated nanocrystal. However, the present phonon renormalization comes from a nonperturbative approach, resulting in a size-dependent DPI coupling strength and therefore can capture the DPI even at nanoscale, becoming a great advantage of this quasi-phonon approach.

In fact, before the formal introduction, classical DPI studies have already hinted at phonon renormalization, due to the drag force nature in the DPI.[16,20,25] This can be better understood from a direct comparison of the DPI with a polaron, where in both cases a drag force leads to the renormalization.[26] An electron moving in materials coupling with a phonon will induce a local polarization known as the polaron (Figure 1b). In the case of the Fröhlich large polaron, the electron−phonon coupling matrix $M(\boldsymbol{q})$ has component $\propto v_q$ where v_q is the electron group velocity.[26] In the case of DPI, due to the similar drag interaction proportional to the velocity (eq 2), it is not difficult to foresee that a phonon can also be renormalized as a quasi-phonon (Figure 1c). Unlike the classical picture in which a phonon collides with a dislocation and then is scattered (Figure 1a), this phonon experiences the long-range dislocation strain field even far away from the dislocation core. This gives the heuristic reason that a quantum field theory of a dislocation capable of describing both its vibrating feature and long-range spatial distribution is more suitable to describe the DPI process than the classical particle-like scattering due to the extended nature of the dislocation.

To study the quantum interaction between a phonon and a dislocation, we adopt a fully quantized field of a dislocation, "dislon", defined in a separate study.[24] A dislon is a quantized collective excitation associated with a dislocation with vibration and strain energy, where the dislocation's definition $\oint \mathrm{d}\mathbf{u} = -\mathbf{b}$ is maintained (see Table 1 for an intuitive comparison with phonon, and see Supporting Information B for the associated formalism). Starting from the second quantized Hamiltonian of the phonon and dislon fields, the total Hamiltonian can be written as (Supporting Information C)

$$\begin{aligned} H &= H_{\mathrm{ph}} + H_{\mathrm{D}} + H_{\mathrm{int}} \\ &= \sum_{\mathbf{k}\lambda} \omega_{\mathbf{k}\lambda}\left(b_{\mathbf{k}\lambda}^{+} b_{\mathbf{k}\lambda} + \frac{1}{2}\right) + \sum_{\kappa} \Omega(\kappa)\left[a_{\kappa}^{+} a_{\kappa} + \frac{1}{2}\right] + H_{\mathrm{int}} \end{aligned} \tag{1}$$

where a_κ and $b_{\mathbf{k}\lambda}$ are dislon and phonon field operators with dispersion $\Omega(\kappa)$and $\omega_{\mathbf{k}\lambda}$, respectively, and $\kappa \equiv k_z$ since the dislocation line is chosen to be along the z-direction.

The interaction between the dislocation and phonon originates from the fact that the total lattice displacement $\mathbf{u}_{\mathrm{tot}}$ is the vector addition of the phonon displacement $\mathbf{u}_{\mathrm{ph}}$ and the dislocation displacement $\mathbf{u}_{\mathrm{dis}}$, i.e., $\mathbf{u}_{\mathrm{tot}} = \mathbf{u}_{\mathrm{ph}} + \mathbf{u}_{\mathrm{dis}}$. This gives a kinetic energy cross term $\dot{\mathbf{u}}_{\mathrm{ph}}\dot{\mathbf{u}}_{\mathrm{dis}}$, harmonic potential cross term $u_{\mathrm{ph}}u_{\mathrm{dis}}$, and anharmonic cross terms $\mathbf{u}_{\mathrm{ph}}{}^{2}\mathbf{u}_{\mathrm{dis}}{}^{1}$ and $\mathbf{u}_{\mathrm{ph}}{}^{1}\mathbf{u}_{\mathrm{dis}}{}^{2}$. Since the anharmonic terms only dominate at high temperature with weak cross terms (Supporting Information I), while the harmonic potential cross term vanishes,[18,27] the dominant term at low temperature is widely accepted to be $\dot{\mathbf{u}}_{ph}\dot{\mathbf{u}}_{dis}{}^{4}$ called fluttering.[17] The corresponding interacting DPI Hamiltonian for a single-mode phonon can be written as (Supporting Information D)

$$\begin{aligned} H_{\mathrm{int}} &= \rho \int \dot{u}_{\mathrm{ph}}(\mathbf{R})\cdot\dot{u}_{\mathrm{D}}(\mathbf{R})\, \mathrm{d}^3\mathbf{R} \\ &= \sum_{\mathbf{k}} \frac{\hbar}{2L}\sqrt{\frac{\rho\omega_{k\lambda}\Omega(\kappa)}{m(\kappa)}}\,(\varepsilon_{\mathbf{k}\lambda}^{*}\cdot F(k))(-b_k^{+} + b_{-k}) \\ &\quad (a_{-\kappa}^{+} - a_{\kappa}) \end{aligned} \tag{2}$$

where ρ is the mass density, $\varepsilon_{\mathbf{k}\lambda}^{*}$ is the phonon polarization vector, $\mathbf{F}(\mathbf{k})$ and $m(\boldsymbol{\kappa})$ are parameters defined in Supporting Information D. By rewriting a dislocation line as an extended quantized field, the static dislocation feature is already incorporated into this formalism since the static case becomes a special case of a full quantized dynamic field. Or rigorously, the definition of a dislocation $\oint d\mathbf{u} = -\mathbf{b}$ is maintained through the dislon field definition, treating the static strain and vibration from an equal footing.[24]

Equations 1 and 2 can be solved by using an infinite-order Green's function method (see Supporting Information G), but is too complicated to directly see the essential physics. To gain more physical intuition onto the influence of dislocations on phonons but to avoid the uncontrolled uncertainty arising from low-order perturbative analysis, we take a nonperturbative functional integral approach,[28] which is capable to treat a strongly interacting system with more physical intuition but without the summation of infinite number of Feynman diagrams. The actions of the noninteracting phonon and dislon field in eq 1 in the Matsubara frequency domain can be written as (see Supporting Information C)

$$\begin{aligned} S_{\mathrm{ph}}(\bar{\phi}, \phi) &= \sum_{n\mathbf{k}} \bar{\phi}_{\mathbf{k}n}(-\mathrm{i}\omega_n + \omega_{\mathbf{k}})\phi_{\mathbf{k}n} \equiv \sum_{n\mathbf{k}} \bar{\phi}_{\mathbf{k}n} {G_{0n\mathbf{k}}}^{-1}\phi_{\mathbf{k}n} \\ S_{\mathrm{D}}(\bar{\chi}, \chi) &= \sum_{n\kappa} \bar{\chi}_{\kappa n}(-\mathrm{i}\omega_n + \Omega(\kappa))\chi_{\kappa n} \end{aligned} \tag{3}$$

where $\omega_n \equiv 2\pi n k_B T$ is the Matsubara frequency, and $\phi_{\mathbf{k}n}$ and $\chi_{\kappa n}$ are the phonon and dislon field, respectively. The DPI action can be written as (see Supporting Information D)

$$\begin{aligned} S_{\mathrm{int}} = \sum_{n\mathbf{k}} \frac{1}{2L}\sqrt{\frac{\rho\omega_k\Omega(\kappa)}{m(\kappa)}}\,\varepsilon_{\mathbf{k}}^{*}\cdot\mathbf{F}(\mathbf{k})(-\bar{\phi}_{\mathbf{k}n}(\chi_{\kappa n} - \bar{\chi}_{-\kappa,-n}) \\ + \phi_{-\mathbf{k}n}(\bar{\chi}_{-\kappa n} - \chi_{\kappa -n})) \end{aligned} \tag{4}$$

In order to eliminate the dislon degree of freedom, the effective phonon action is defined by integrating out the dislon degree of freedom as

$$S_{\mathrm{eff}}(\bar{\phi}, \phi) \equiv S_{\mathrm{ph}}(\bar{\phi}, \phi) - \log\left[\int D(\bar{\chi}, \chi)\, \mathrm{e}^{-S_D - S_{\mathrm{int}}}\right] \tag{5}$$

The effective action can finally be simplified using the Keldysh rotation[29] and matrix operation as (see Supporting Information E)

$$\begin{aligned} S_{\mathrm{eff}}(\bar{\varphi}, \varphi) &= \sum_{n\mathbf{k}\mathbf{k}'} \frac{1}{2}\bar{\varphi}_{n\mathbf{k}'}\Big[{G_{0n\mathbf{k}}}^{-1}\delta_{\mathbf{k}\mathbf{k}'} - 2J_{n\kappa}\delta_{\kappa\kappa'}g_{\mathbf{k}}^{*}g_{\mathbf{k}'} \\ &\quad + \sqrt{{G_{0n\mathbf{k}}}^{-2}\delta_{\mathbf{k}\mathbf{k}'} + 4(J_{n\kappa}\delta_{\kappa\kappa'}g_{\mathbf{k}}^{*}g_{\mathbf{k}'})^2}\Big]\varphi_{n\mathbf{k}} \\ &\equiv \sum_{n\mathbf{k}\mathbf{k}'} \bar{\varphi}_{n\mathbf{k}'}{G_{n\mathbf{k}'\mathbf{k}}}^{-1}\varphi_{n\mathbf{k}} \end{aligned} \tag{6}$$

DOI: 10.1021/acs.nanolett.6b04756
Nano Lett. 2017, 17, 1587−1594

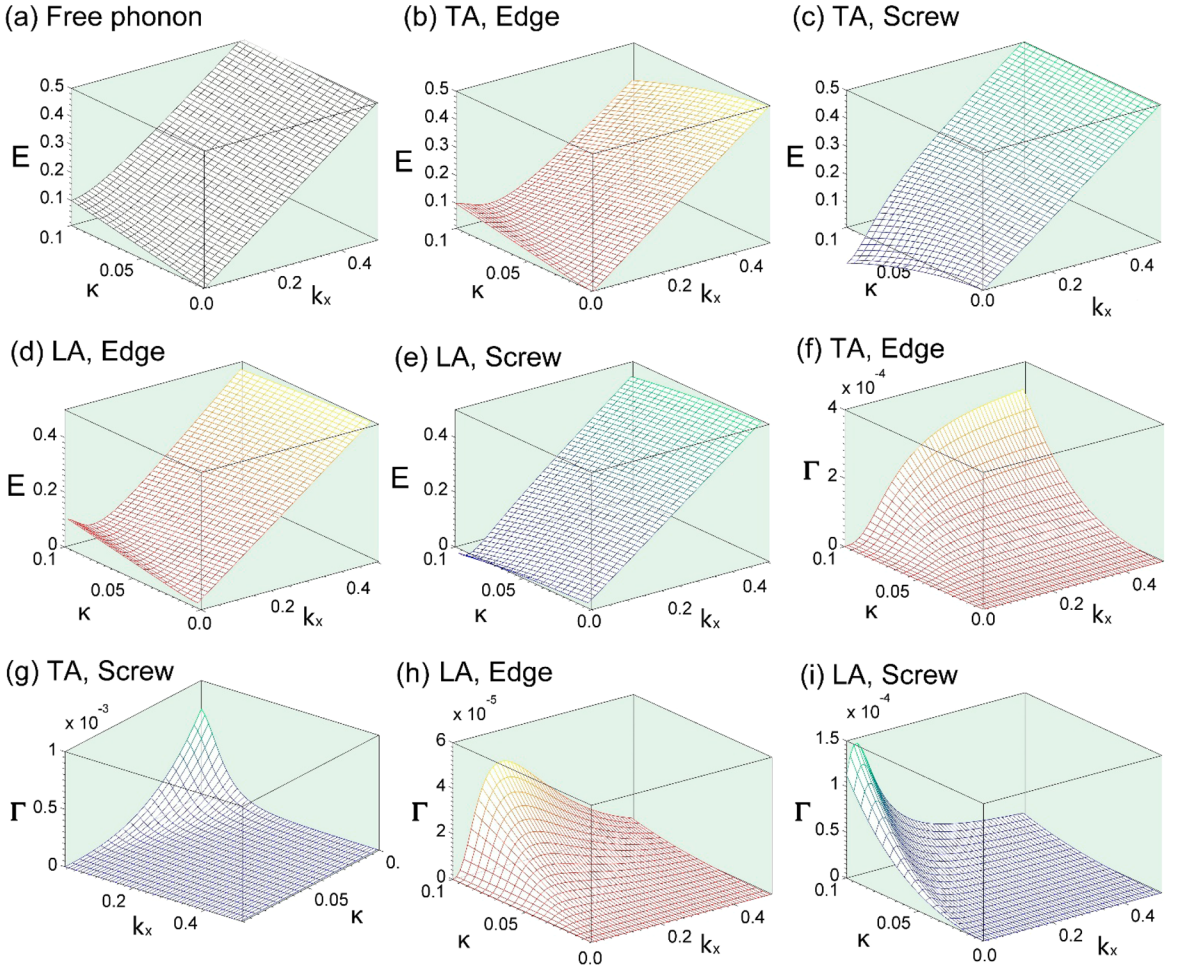

Figure 2. Numerical diagonalization of quasi-phonon spectra, when a linear-dispersive free phonon (a) interacts with an edge (red; b,d,f,h) or a screw (blue; c,e,g,i) dislocation. The quasi-phonon energies (b−e) are lowered upon renormalization compared with a bare phonon (a), and the energy shift is greater at high κ magnitude, which is reasonable since higher κ indicates a larger dislocation vibration hence larger dislon excitation. The quasi-phonon relaxation rates Γ(f−i) show fruitful structures beyond the perturbation theories where only monotonic changes occur. On one hand, whether relaxation rate Γ increases or decreases as a function of phonon wavevector k_x depends on dislocation type (f vs g). However, the resonance scattering where Γ is peaked can be seen directly from this nonperturbative approach (h,i).

with $g_{\mathbf{k}} = (\varepsilon_{\mathbf{k}}^{*}\cdot\mathbf{F}(\mathbf{k}))\sqrt{\omega_{\mathbf{k}}}$, $R(\kappa) = \frac{\rho}{4A}\frac{\Omega(\kappa)}{m(\kappa)}$, and φ denotes the effective phonon field to distinguish from the bare phonon field ϕ, where $J_{n\kappa} \equiv \frac{R(\kappa)\Omega(\kappa)}{\omega_n^2+\Omega^2(\kappa)}$is the phonon−dislon coupling strength, containing both dynamic scattering $\omega_n \neq 0$ and static scattering $\omega_n = 0$ contributions. $G_{n\mathbf{kk}}{}^{-1}$ is the expression inside the square brackets in eq 6, giving the scattering amplitude of an incoming phonon k, after being scattered by a dislocation, resulting in an outing phonon $\mathbf{k}'$. Equation 6 is the main result of this theory and contains rich physics: (a) When $J_{\kappa n} = 0$ (no DPI), the effective action eq 6 directly reduces to the free phonon action eq 3. (b) The $\boldsymbol{\delta}_{\kappa\kappa'}$ term indicates that only two phonons with identical z-momentum can be coupled by a dislocation, which makes good physical sense. (c) It treats static and dynamic scattering from an equal footing. (d) Most importantly, eq 6 shows that a phonon is dressed to a quasi-phonon upon interaction with a dislocation, i.e., $\boldsymbol{\omega}_{\mathbf{k}} \rightarrow \boldsymbol{E}_{\mathbf{k}} + \mathrm{i}\boldsymbol{\Gamma}_{\mathbf{k}}$. To see this, we note that eq 6 contains many off-diagonal $\mathbf{k} \neq \mathbf{k}'$ elements, and $G_{n\mathbf{k}'\mathbf{k}}{}^{-1} = -i\omega_n + H_{n\mathbf{k}'\mathbf{k}}$ can be understood as an inverse Green's function, in which $H_{n\mathbf{k}'\mathbf{k}}$ is the off-diagonal Hamiltonian. To obtain the quasi-phonon spectra, a diagonalization procedure shall be performed:

$$
\begin{aligned}
S_{\mathrm{eff}}(\bar{\varphi}, \varphi) &= \sum_{n\mathbf{k}\mathbf{k}'} \bar{\varphi}_{n\mathbf{k}'} G_{n\mathbf{k}'\mathbf{k}}{}^{-1} \varphi_{n\mathbf{k}} \\
&= \sum_{n\mathbf{k}\mathbf{k}'} \bar{\varphi}_{n\mathbf{k}'}(-\mathrm{i}\omega_n + H_{n\mathbf{k}'\mathbf{k}})\varphi_{n\mathbf{k}} \\
&\approx \sum_{n\mathbf{k}} \bar{\varphi}'_{n\mathbf{k}}(-\mathrm{i}\omega_n + E_{\mathbf{k}} + \mathrm{i}\Gamma_{\mathbf{k}})\varphi'_{n\mathbf{k}}
\end{aligned}
\tag{7}
$$

As a very rough approximation, the diagonal matrix element in eq 6 gives the renormalized quasi-phonon energy E_{k} while the off-diagonal part gives quasi-phonon relaxation rate $\Gamma_{\mathbf{k}}$ in the acoustic limit (see Supporting Information F),

$$
\begin{aligned}
&E_{\mathbf{k}} \approx \omega_{\mathbf{k}} - 2J_{n\kappa}|g_{\mathbf{k}}|^2 \\
&\Gamma_{\mathbf{k}} \approx 2\sum_{\mathbf{k}'} J_{n\kappa}\delta_{\kappa\kappa'} g_{\mathbf{k}}^{*} g_{\mathbf{k}'} \begin{cases} \approx (J_0/\pi)b^2\omega, & \text{static} \\ \propto 1/\omega, & \text{dynamic} \end{cases}
\end{aligned}
\tag{8}
$$

For the static scattering, eq 8 is consistent with the classical Carruthers' result[3] $1/\tau_s \approx N_{\mathrm{d}}\gamma^2 b^2\omega$ where γ is the Grüneisen parameter.

For dynamic scattering, for a given dislon excitation at small κ, eq 8 gives $J_{\kappa n} \propto 1/\omega^2$ after analytical continuation. This

DOI: 10.1021/acs.nanolett.6b04756
Nano Lett. 2017, 17, 1587−1594

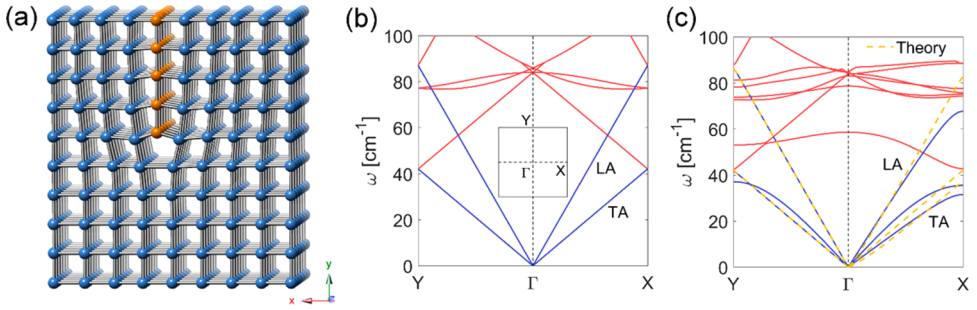

Figure 3. Lattice dynamics simulation of a dislocated cubic supercell. (a) A 10 × 10 supercell configuration showing the schematics for lattice dynamics simulation; in this simulation, a larger 30 × 30 supercell is used. The computed phonon spectra without (b) and with (c) a dislocation in a supercell Brillouin zone. It is clearly seen that phonon energies are experiencing an anisotropic shift, where the dispersion mostly changes along Γ−X direction but not Γ−Y direction, accompanied by a reduction of phonon group velocity (see for instance, the LA mode). This is in excellent agreement with the effective quasi-phonon theory prediction using eq 6 (yellow dashed lines), where the phonon dispersion does not change along Γ−Y direction, but the group velocity is dropped along Γ−X direction. In (c), the splitting of TA modes along Γ−Y direction is not captured since it may be caused by the interaction between supercells instead of one single dislocation, while along Γ−X direction, the splitting is captured since it is caused by phonon polarization effect.

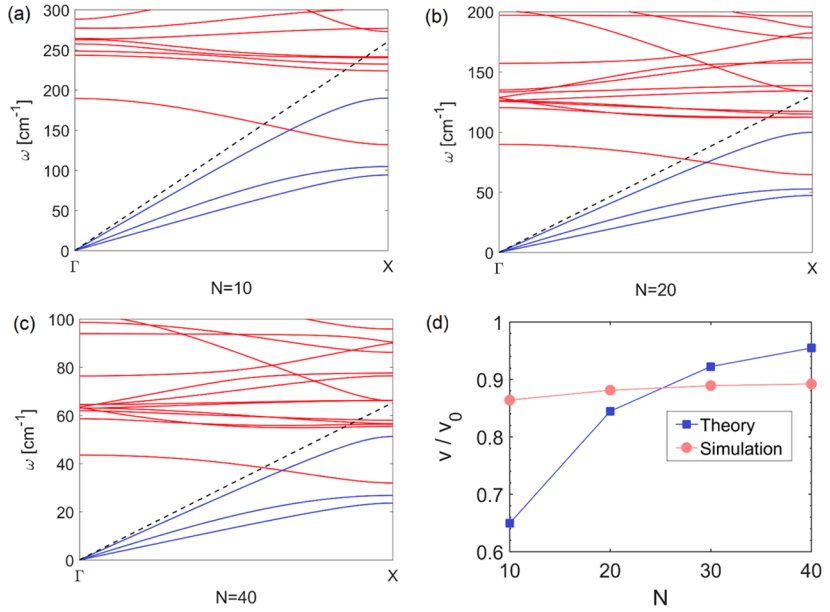

Figure 4. Classical size effect of the phonon spectra. (a−c) The lattice dynamics simulation of the phonon spectra at various $N \times N$ supercells (N = 10, 20, 40; results for N = 30 are in Figure 3). Since there is no phonon energy shift along Γ−Y direction, only the spectra long Γ−X direction are plotted. The black-dashed lines are the LA mode without dislocation as a comparison. (d) The ratio of the LA mode sound velocity with the presence of dislocation (v) to the velocity without dislocation (v_0), at various supercell sizes. Both the lattice dynamics simulation (red curve) and the quasi-phonon theory (blue curve) show the same trend qualitatively, which is a classical size effect of group velocity reduction, where smaller supercell gives smaller grow velocity. To perform the comparison, a κ = 0.01 value is chosen. When the cell size grows larger, the ratio approaches to the bulk value (v/v_0 = 1). The quantitative difference, such as a stronger size dependence from the quasi-phonon theory is caused by different boundary conditions. Unlike the simulation that has periodic boundary condition, the theory considers only one dislocation, leading to the faster fading of the DPI strength when the supercell size is larger.

finally leads to $1/\tau_d \propto 1/\omega$, which is consistent with the dynamic scattering results where the relaxation rate is independent of the Burgers vector **b**.[15,18,30]

Intriguingly, compared to the perturbation theories that contain only an averaged, structureless simple ω-dependence of relaxation rate Γ_k as in eq 8, eq 6 has additional power to consider the anisotropic **k**-dependence of the scattering process and hence is able to capture the effects caused by the dislocation type, anisotropy, and DPI resonance, as shown in Figure 2. Compared to the free phonon with linear dispersion $\omega_k = v_s k$, where the shear velocity v_s = 1 (Figure 2a), the renormalized quasi-phonon dispersions and the quasi-phonon lifetimes are plotted in Figure 2b−e and Figure 2f−i, respectively. The results are obtained by numerically diagonalizing eq 6. In all computations, we have assumed that the Debye wavenumber k_D = 1, the sample area A = 1, and the Poisson ratio ν = 0.3, and we have defined the xz-plane as the slip plane (all are dimensionless for numerical comparisons). In all cases in Figures 2b−e, it can be seen clearly that there is a phonon energy renormalization effect, where the phonon energy experiences a red-shift upon renormalization, indicating a drop of group velocity with the presence of dislocation. This effect is qualitatively consistent with the estimation of eq 8 and lattice dynamics simulation in Figures 3 and 4. The renormalized phonon dispersions are plotted for both an edge dislocation (**b** = [1 0 0], Figure 2b,d) and a screw

DOI: 10.1021/acs.nanolett.6b04756
Nano Lett. 2017, 17, 1587−1594

dislocation ($\mathbf{b}$ = [0 0 1], Figure 2c,e), in both transverse mode (Figure 2b,c, ε_k = [0 1 0], $\mathbf{k} \perp \varepsilon_\mathbf{k}$) and longitudinal mode (Figure 2d,e, $\varepsilon_\mathbf{k}$ = [1 1 1], $\mathbf{k} \parallel \varepsilon_\mathbf{k}$). It can also be seen that a larger change of the quasi-phonon energy is expected at high κ magnitude, which is reasonable since higher κ indicates dislocation that is vibrating strongly.

Figure 2f–i shows the quasi-phonon relaxation rate $\Gamma_\mathbf{k}$ of edge (Figure 2f,h) and screw (Figure 2g,i) dislocations, with the incidence of transverse (Figure 2f,g) and longitudinal phonons (Figure 2h,i). On one hand, for the transverse incidence, at given κ, $\Gamma_\mathbf{k}$ increases monotonically with k_x for an edge dislocation (Figure 2f), making the relaxation process more like static-strain relaxation ($\Gamma \propto 1/\omega$, discussed in Supporting Information F), but decreases with k_x for a screw dislocation (Figure 2g), making the relaxation process resemble a vibrating-string relaxation ($\Gamma \propto 1/\omega$, discussed in Supporting Information F). In other words, even for the same type of phonon incidence, the DPI can be dominated by either dynamic or static scattering, depending on the dislocation type. This fact can only be revealed when the anisotropic $\mathbf{k}$-dependence is taken into account properly and is completely ignored in previous theoretical treatments where only the explicit ω-dependence was considered, leading to a much simpler monotonic phonon relaxation structure regardless of dislocation type. On the other hand, for the longitudinal instance, $\Gamma_\mathbf{k}$ shows a peaked value at certain k values (Figure 2h,i), which can be understood as a resonant DPI process. Such resonance scattering can never be obtained through any perturbative approach, where $\Gamma_\mathbf{k}$ can only vary monotonically with ω.

In the past, phonon spectra are assumed to be unchanged in almost all DPI studies. This assumption is plausible for large samples due to the $1/A$ prefactor in the coupling strength $J_{\kappa n}$, but breaks down for small samples where dislocation has a higher weight, such as the case of phonon transport at the nanoscale. To further validate the prediction of eq 6 and to see whether this anisotropic energy renormalization is possibly observable, we performed a lattice dynamics simulation to compute the phonon dispersion (see Lattice Dynamics Simulation). Compared with the nondislocated dispersion (Figure 3b), the anisotropic energy red-shift (for instance, no shift along the Γ–Y direction, shift from 85 to 70 cm^{-1} for the LA mode along the Γ–X direction) and the reduction of group velocity by lattice dynamics simulation are also correctly predicted through the effective theory eq 6 (yellow dashed lines in Figure 3c). It is also worthwhile mentioning that, in either the static DPI approach or dynamic DPI approach, the phonon spectra are assumed to be fixed. This indicates a breakdown of both approaches when applied to the nanoscale, where a >10% change of phonon energy is expected with the presence of a dislocation (Figure 3c). However, the present phonon renormalization theory can deal with the nanoscale DPI, as shown in Figure 4. At various simulated sample cell sizes (Figure 4a–c), the phonon spectra are clearly different from one to the other, as is expected physically. This finally results in a size effect of the acoustic sound velocity (Figure 4d), which approaches to the bulk value, then the sample is getting bigger. It is also worth mentioning that the change of phonon spectra in a confined environment has recently been observed in an experimental study.[31] Since we are dealing with one single dislocation without periodic boundary condition, the size dependence in the theory is more drastic than the simulation where periodic boundary condition is assumed.

All of the above DPI mechanisms are dominant at very low temperature where anharmonic phonon–phonon interaction is weak. Dislocations may also reduce the thermal conductivity above the thermal conductivity maximum temperature.[12,15,30] This is explained as contributions beyond the sole dislocation, such as dislocation dipoles[15] or stacking faults.[30] In such cases, the question whether this phenomenon is intrinsic (meaning that such phenomenon can be induced by dislocation itself) or is extrinsic (such as stacking fault scattering) has not been resolved. In the present work, by using the quasi-phonon picture, it can be shown directly that a dislocation can actually reduce thermal conductivity at all temperatures due to the reduction of sound velocity. From eq 6, the Matsubara Green function can be written as

$$G_{n\mathbf{kp}} \equiv G_{n\mathbf{k},m\mathbf{p}} = \langle \varphi_{n\mathbf{k}} \bar{\varphi}_{m\mathbf{p}} \rangle = \frac{\delta_{mn} G_{0n\mathbf{k}}}{\frac{1}{2}\delta_{\mathbf{pk}} - J_{n\kappa} G_{0n\mathbf{k}} \delta_{\kappa p_z} g^*_\mathbf{k} g_\mathbf{p} + \sqrt{\frac{1}{4}\delta_{\mathbf{pk}} + (J_{n\kappa} G_{0n\mathbf{k}} \delta_{\kappa p_z} g^*_\mathbf{k} g_\mathbf{p})^2}} \tag{9}$$

The corresponding thermal conductivity Kubo formula compatible with eq 9 can then be computed as (see Supporting Information H)

$$k(T) = -\frac{k_B \beta^2}{12\pi V} \sum_{\mathbf{kp}} \mathbf{v}_\mathbf{k} \cdot \mathbf{v}_\mathbf{p} E_\mathbf{k} E_\mathbf{p} \int_{-\infty}^{+\infty} d\omega \times \frac{[G^R_{\mathbf{kp}}(\omega) - G^A_{\mathbf{kp}}(\omega)][G^R_{\mathbf{pk}}(\omega) - G^A_{\mathbf{pk}}(\omega)]}{[\exp(\beta\omega) - 1]^2} \tag{10}$$

where $\mathbf{v}_\mathbf{k} \equiv \partial E_\mathbf{k}/\partial \mathbf{k}$ is the quasi-phonon group velocity, $G^R(\omega)$ and $G^A(\omega)$ are the retarded and advanced Green functions obtained by analytical continuation of eq 9. This indicates that the impact of dislocation ranges in all temperatures is due to the reduction of the group velocity $\mathbf{v}_\mathbf{k}$. To the best of our knowledge, this is also the first time the change of the phonon dispersion caused by DPI is considered in dealing with thermal transport problems.

The effective theory approach using eq 6 resolves another problem related to symmetry breaking. Phonons are well-defined within the first Brillouin zone as a result of lattice translational symmetry. The long-range strain field caused by dislocations breaks lattice periodicity and thereby blurs the definition of crystal momentum $\mathbf{k}$ as a good quantum number. In the process of phonon renormalization, according to eq 5, the symmetry-breaking dislon field χ is integrated out, the effect of the dislocation on the phonons can be discussed using weakly interacting quasi-phonons within the restored first Brillouin zone using the effective theory approach.

Since the effective quasi-phonon theory is based on a continuum elastic theory of a crystal dislocation, we must be cautious in applying the theory to a nanosized crystal, where certain conditions have to be met in order for the quasi-phonon theory to be valid. The first condition deals with the dislocation core size. Since the linear elasticity theory remains valid except at the dislocation core region,[32−36] the crystal size L must be at least greater than the dislocation core radius r_0, i.e., $L \gg r_0 = \frac{\mu b^2}{8\pi^2\gamma}$, where γ represents the specific surface energy of the crystal.[37] The second condition deals with phonon–phonon anharmonicity, which increases as a function of temperature. As long as $\Gamma_\mathbf{k} \gg \Gamma_{\mathbf{k},an}$, where $\Gamma_{\mathbf{k},an}$ is the relaxation rate caused by anharmonicity,[38,39] the present quasi-phonon

DOI: 10.1021/acs.nanolett.6b04756
Nano Lett. 2017, 17, 1587–1594

theory still produces a good approximation due to relatively weaker anharmonicity. In addition, the phonon−dislocation anharmonic effect is shown to be weak (Supporting Information I), so that we could focus on the fluttering effect without considering the anharmonic effects in the present DPI study. The third condition deals with boundary scattering, where the phonon−crystal surface scattering is increased due to the increase surface to bulk ratio. In this scenario, $\Gamma_k \gg \Gamma_B$, where Γ_B is the relaxation rate from boundary scattering, needs to be satisfied in order for the quasi-phonon theory to remain valid. In a simple estimation, Γ_B is given by Casimir limit $\Gamma_B = \frac{v_g}{L}$ in which v_g is the phonon group velocity.[40] The fourth condition deals with the independent-dislocation assumption, where strongly interacting dislocations may dominate the phonon−dislocation interaction at high dislocation density. According to the present simulation, at $N = 40$ (corresponding to interdislocation distance ∼9 nm and dislocation density $\sim 10^{12}/\mathrm{cm}^2$), the dislocation−dislocation interaction effect still persists, hence an independent dislocation assumption shall be valid when dislocation density is much lower than $\sim 10^{12}/\mathrm{cm}^2$. As long as all above conditions are met, the current quasi-phonon theory can be considered as a good approach in describing the DPI at nanoscale.

To summarize, we have shown that the dislocation−phonon interaction has the nature of phonon renormalization. This feature has been overlooked in previous perturbative analysis and only becomes clear through a nonperturbative approach as is adopted in the present work. A renormalized phonon unifies the decades-long debate between static and dynamic dislocation−phonon scattering mechanisms. In particular, both approaches break down at the nanoscale, while the renormalized phonon theory remains valid by capturing the size effect. By treating a dislocation line as a quantized field, both its long-range nature and vibrational properties are automatically captured. In the present study, we focus on providing a theoretical framework, but do not intend to seek quantitative agreement with realistic materials, for the following reasons: (a) The classical fluttering model[18] prior to quantization has already obtained excellent agreement with experiments. (b) The quasi-phonon relaxation rate is shown to be reducible to classical results of DPI relaxation rate. (c) Experimental agreement of $k(T)$ is not a sufficient condition to reveal the nature of dislocation induced thermal resistivity since the $\mathbf{k}$-dependence of the relaxation is ignored in classical theories, thereby resulting in a simpler ω-dependence. Instead, we focus on the multiple possibilities of what a quantized dislocation, "dislon", can bring. It opens up an unexplored territory of the dislocation−phonon relaxation structure, depending on energy, momentum, anisotropy, and dislocation types and phonon modes. The picture of the renormalized phonon provides insights not only as a conceptual breakthrough but also as a framework to study the influence of dislocation on the thermal properties of a nanomaterial from a fundamental level.

Lattice Dynamics Simulation. We perform lattice dynamics simulation with four supercells with size $N \times N \times 1$ ($N = 10, 20, 30, 40$) with a hypothetical simple cubic crystal with lattice parameter $a = 2.2$ Å, Poisson ratio $\nu = 0$, Young's modulus 540 GPa, and creating an edge dislocation with Burgers vector $\mathbf{b} = a\hat{x}$ (Figure 3a). This theory does not intend to fully reproduce the existing theory since it contains only one dislocation while the simulation is a periodic dislocation array. To perform the comparison between the theory and simulation the following parameters were used: a shear velocity $v_s = 1$, temperature $T = 1$, Poisson ratio $\nu = 0$, Matsubara index $n = 0$, and dislon excitation $\kappa = 0.01$. Other values may result in some quantitative difference, but the size effect of phonon group velocity reduction always exists.

■ ASSOCIATED CONTENT

Supporting Information

The Supporting Information is available free of charge on the ACS Publications website at DOI: 10.1021/acs.nanolett.6b04756.

Reason for breakdown of the perturbation approach, a brief review of quantized dislocation ("dislon") theory, derivation of effective action of phonon−dislon interaction, derivation of effective phonon action theory, computation of phonon−dislon interaction relaxation time, method to compute thermal conductivity based on our formalism, and estimation of the contribution from anharmonicity (PDF)

■ AUTHOR INFORMATION

Corresponding Authors

*E-mail: mingda@mit.edu (M.L.).
*E-mail: gchen2@mit.edu (G.C.).

ORCID

Mingda Li: 0000-0002-7055-6368
Zhiwei Ding: 0000-0002-2612-7750

Author Contributions

M.L. conceived and developed the research along with G.C. and M.S.D. M.L. performed the nonperturbative theoretical calculations with the help of H.L. Z.D. and J.Z. performed the lattice dynamics simulation. Q.P. performed infinite-order Green's functions calculation and checked the calculation along with Y.Z. M.L., M.S.D., and G.C. wrote the manuscript with contributions from all authors.

Notes

The authors declare no competing financial interest.

■ ACKNOWLEDGMENTS

M.L. would thank W. Cui, J. Mendoza, S. Huang, and S. Huberman for their helpful discussions. M.L., M.S.D., and G.C. would like to thank support by S^3TEC, an Energy Frontier Research Center funded by U.S. Department of Energy (DOE), Office of Basic Energy Sciences (BES) under Award No. DE-SC0001299/DE-FG02-09ER46577 (for fundamental research in thermoelectric transport) and DARPA MATRIX Program Contract HR0011-16-2-0041 (for developing and applying the simulation codes). Q.M. and Y.Z. are supported by DOE-BES, Materials Science and Engineering Division under contract No. DE-SC0012704. H.L. is supported in part by funds provided by the DOE cooperative research agreement DE-SC0012567.

■ REFERENCES

(1) Nabarro, F. R. N. *Theory of Crystal Dislocations*; Clarendon P.: Oxford, 1967; p xviii.
(2) Klemens, P. G. *Proc. Phys. Soc., London, Sect. A* **1955**, *68* (12), 1113.
(3) Carruthers, P. *Rev. Mod. Phys.* **1961**, *33* (1), 92−138.
(4) Maurel, A.; Mercier, J.-F.; Lund, F. *Phys. Rev. B: Condens. Matter Mater. Phys.* **2004**, *70* (2), 024303.

DOI: 10.1021/acs.nanolett.6b04756
Nano Lett. 2017, 17, 1587−1594

(5) Sproull, R. L.; Moss, M.; Weinstock, H. *J. Appl. Phys.* **1959**, *30* (3), 334−337.
(6) Cotts, E. J.; Miliotis, D. M.; Anderson, A. C. *Phys. Rev. B: Condens. Matter Mater. Phys.* **1981**, *24* (12), 7336−7341.
(7) Northrop, G. A.; Cotts, E. J.; Anderson, A. C.; Wolfe, J. P. *Phys. Rev. B: Condens. Matter Mater. Phys.* **1983**, *27* (10), 6395−6408.
(8) Yang, I. S.; Anderson, A. C.; Kim, Y. S.; Cotts, E. J. *Phys. Rev. B: Condens. Matter Mater. Phys.* **1989**, *40* (2), 1297−1300.
(9) Bross, H. *Phys. Status Solidi B* **1962**, *2* (5), 481−516.
(10) Eckhardt, D.; Wasserbäch, W. *Philos. Mag. A* **1978**, *37* (5), 621−637.
(11) Wasserbach, W. *Phys. Status Solidi B* **1985**, *128* (2), 453−466.
(12) Sato, M.; Sumino, K. *J. Phys. Soc. Jpn.* **1974**, *36* (4), 1075−1083.
(13) Nabarro, F. R. N. *Proc. R. Soc. London, Ser. A* **1951**, *209* (1097), 278−290.
(14) Eshelby, J. D. *Proc. R. Soc. London, Ser. A* **1962**, *266* (1325), 222−246.
(15) Kneeze, G. A.; Granato, A. V. *Phys. Rev. B: Condens. Matter Mater. Phys.* **1982**, *25* (4), 2851−2866.
(16) Al'Shitz, V.; Indenbom, V. *Physics-Uspekhi* **1975**, *18* (1), 1−20.
(17) Ninomiya, T. *J. Phys. Soc. Jpn.* **1974**, *36* (2), 399−405.
(18) Ninomiya, T. *J. Phys. Soc. Jpn.* **1968**, *25* (3), 830−840.
(19) Granato, A.; Lücke, K. *J. Appl. Phys.* **1956**, *27* (6), 583.
(20) Garber, J. A.; Granato, A. V. *J. Phys. Chem. Solids* **1970**, *31* (8), 1863−1867.
(21) Maurel, A. s.; Mercier, J.-F. o.; Lund, F. *J. Acoust. Soc. Am.* **2004**, *115* (6), 2773.
(22) Maurel, A.; Lund, F.; Barra, F.; Pagneux, V. *MRS Online Proc. Libr.* **2012**, *1404*, 341.
(23) Rodríguez, N.; Maurel, A. s.; Pagneux, V.; Barra, F.; Lund, F. *J. Appl. Phys.* **2009**, *106* (5), 054910.
(24) Li, M.; Cui, W.; Dresselhaus, M. S.; Chen, G. Canonical quantization of crystal dislocation and electron-dislocation scattering in an isotropic medium. *New J. Phys.* **2017**, *19*, 013033.
(25) Brailsford, A. D. *J. Appl. Phys.* **1970**, *41* (11), 4439.
(26) Mahan, G. D. *Many-Particle Physics*,. 3rd ed.; Kluwer Academic/Plenum Publishers: New York, 2000; p xii.
(27) Ninomiya, T. *J. Res. Nbs a Phys. Ch* **1969**, *A 73* (5), 544.
(28) Negele, J. W.; Orland, H. *Quantum Many-Particle Systems*; Addison-Wesley Pub. Co.: Redwood City, CA, 1988; p xviii.
(29) Kamenev, A. Many-body theory of non-equilibrium systems. arXiv:cond-mat/0412296, 2004.
(30) Singh, B. K.; Menon, V. J.; Sood, K. C. *Phys. Rev. B: Condens. Matter Mater. Phys.* **2006**, *74* (18), 184302.
(31) Kargar, F.; Debnath, B.; Kakko, J. P.; Saynatjoki, A.; Lipsanen, H.; Nika, D. L.; Lake, R. K.; Balandin, A. A. *Nat. Commun.* **2016**, *7*, 13400.
(32) Curtin, W. A.; Miller, R. E. *Modell. Simul. Mater. Sci. Eng.* **2003**, *11* (3), R33.
(33) Li, J.; Ngan, A. H. W.; Gumbsch, P. *Acta Mater.* **2003**, *51* (19), 5711−5742.
(34) Clouet, E.; Garruchet, S.; Nguyen, H.; Perez, M.; Becquart, C. S. *Acta Mater.* **2008**, *56* (14), 3450−3460.
(35) Dontsova, E. Understanding of edge and screw dislocations in nanostructures by modeling and simulations, University of Minnesota, 2013.
(36) Webb, E. B.; Zimmerman, J. A.; Seel, S. C. *Mathematics and Mechanics of Solids* **2008**, *13* (3−4), 221−266.
(37) Hirth, J. P.; Lothe, J. *Theory of Dislocations*, 2nd ed.; Krieger Pub. Co., Malabar, FL, 1992; p xii.
(38) Ziman, J. M. *Electrons and Phonons: the Theory of Transport Phenomena in Solids*; Clarendon Press and Oxford University Press: New York, 2001; p xiv.
(39) Mendoza, J.; Chen, G. *Nano Lett.* **2016**, *16* (12), 7616−7620.
(40) Zou, J.; Balandin, A. *J. Appl. Phys.* **2001**, *89* (5), 2932−2938.
(41) Li, M.; Song, Q.; Dresselhaus, M. S.; Chen, G. Three-dimensional non-Bosonic non-Fermionic quasiparticle through a quantized topological defect of crystal dislocation. ArXiv e-prints 1608.07820, 2016.

DOI: 10.1021/acs.nanolett.6b04756
Nano Lett. 2017, 17, 1587−1594